

# The Resonance Peak in Sr<sub>2</sub>RuO<sub>4</sub>: Signature of Spin Triplet Pairing

Dirk K. Morr<sup>1</sup>, Peter F. Trautman<sup>1,2</sup>, and Matthias J. Graf<sup>1</sup>

<sup>1</sup> *Theoretical Division, MS B262, Los Alamos National Laboratory, Los Alamos, NM 87545*

<sup>2</sup> *Baylor University, Waco, TX 76798*

(November 4, 2018)

We study the dynamical spin susceptibility,  $\chi(\mathbf{q}, \omega)$ , in the normal and superconducting state of Sr<sub>2</sub>RuO<sub>4</sub>. In the normal state, we find a peak in the vicinity of  $\mathbf{Q}_i \simeq (0.72\pi, 0.72\pi)$  in agreement with recent inelastic neutron scattering (INS) experiments. We predict that for spin triplet pairing in the superconducting state a *resonance peak* appears in the out-of-plane component of  $\chi$ , but is absent in the in-plane component. In contrast, no resonance peak is expected for spin singlet pairing.

PACS numbers: 74.25.-q, 74.25.Ha, 74.70.-b

The superconducting (SC) state of Sr<sub>2</sub>RuO<sub>4</sub> has been the focus of intense experimental and theoretical research over the last few years. Sr<sub>2</sub>RuO<sub>4</sub> is isostructural with the high-temperature superconductor (HTSC) La<sub>2-x</sub>Sr<sub>x</sub>CuO<sub>4</sub> and is the only known layered perovskite which is superconducting in the absence of Cu [1]. Understanding the pairing mechanism in Sr<sub>2</sub>RuO<sub>4</sub> could therefore provide important insight into the origin of unconventional superconductivity in general, and that of the HTSC in particular. Since a related compound, SrRuO<sub>3</sub>, is a ferromagnet, it was suggested [2,3] that Sr<sub>2</sub>RuO<sub>4</sub> is a triplet superconductor in which the pairing is mediated by ferromagnetic paramagnons. Experimental support for spin triplet pairing comes from Knight shift (KS) [4] and elastic neutron scattering (ENS) measurements [5], while  $\mu$ SR [6] provides evidence for a broken time-reversal symmetry in the SC state. However, the momentum dependence of the superconducting gap is still unclear. While originally a *p*-wave symmetry, belonging to the  $E_u$  representation of the  $D_{4h}$  point group, was proposed for the superconducting gap [2,7],  $\Delta(\mathbf{k}) \sim k_x + ik_y$ , recent specific heat [8], thermal conductivity [9], penetration depth [10], and nuclear magnetic resonance [11] experiments suggest the presence of line nodes in  $\Delta(\mathbf{k})$  and thus pairing with higher orbital momentum.

The spin susceptibility,  $\chi(\mathbf{q}, \omega)$ , is an important input parameter for any theory ascribing the pairing mechanism in Sr<sub>2</sub>RuO<sub>4</sub> to the exchange of spin fluctuations. In this letter we present a scenario for the momentum and frequency dependence of  $\chi(\mathbf{q}, \omega)$ , both in the normal and superconducting state. In the normal state, we find a peak in  $\text{Im } \chi$  whose momentum position is close to that reported by Sidis *et al.* [12] in inelastic neutron scattering (INS) experiments. Our results for  $\text{Re } \chi$  agree with the prediction by Mazin and Singh [13] of a peak in the normal-state static susceptibility,  $\chi(\mathbf{q}, \omega = 0)$ , around  $\mathbf{q} = (2\pi/3, 2\pi/3)$ . We show that for triplet pairing in the superconducting state the in-plane,  $\chi_{\pm} = (\chi_{xx} + \chi_{yy})/2$ , and out-of-plane,  $\chi_{zz}$ , components of the dynamic spin susceptibility are qualitatively different. In particular, we predict that a *resonance peak*, similar to the one observed in the HTSC [14], appears in  $\chi_{zz}$ , but is absent in  $\chi_{\pm}$ . Since no resonance peak exists for spin singlet pairing, it is an important signature of spin triplet su-

perconductivity.

Contributions to the dynamic spin susceptibility in Sr<sub>2</sub>RuO<sub>4</sub> come from three electronic bands which are derived from the Ru 4d *xy*, *xz*, and *yz*-orbitals. A comparison of angle-resolved photoemission (ARPES) [15] and de Haas-van Alphen (dHvA) [16] experiments with band-structure calculations [17] shows a substantial hybridization only between the *xz*- and *yz*-orbitals, with a resulting hole-like ( $\alpha$ -band) and electron-like Fermi surface (FS) ( $\beta$ -band), while the decoupled *xy*-orbitals give rise to the electron-like  $\gamma$ -band [18]. Thus the electronic structure of Sr<sub>2</sub>RuO<sub>4</sub> can be described by the tight-binding Hamiltonian

$$\mathcal{H} = \sum_{\mathbf{k}, \sigma} \epsilon_{\mathbf{k}}^{xy} c_{\mathbf{k}, \sigma}^{\dagger} c_{\mathbf{k}, \sigma} + \sum_{\mathbf{k}, \sigma} \epsilon_{\mathbf{k}}^{xz} a_{\mathbf{k}, \sigma}^{\dagger} a_{\mathbf{k}, \sigma} + \sum_{\mathbf{k}, \sigma} \epsilon_{\mathbf{k}}^{yz} b_{\mathbf{k}, \sigma}^{\dagger} b_{\mathbf{k}, \sigma} - \sum_{\mathbf{k}, \sigma} \left( t_{\perp} a_{\mathbf{k}, \sigma}^{\dagger} b_{\mathbf{k}, \sigma} + h.c. \right), \quad (1)$$

where  $c_{\mathbf{k}}^{\dagger}, a_{\mathbf{k}}^{\dagger}, b_{\mathbf{k}}^{\dagger}$  are the fermionic creation operators in the *xy*, *xz*, and *yz*-bands, with spin  $\sigma$ , respectively. The normal state tight-binding dispersions are given by [17]

$$\epsilon_{\mathbf{k}}^i = -2t_x \cos k_x - 2t_y \cos k_y + 4t' \cos k_x \cos k_y - \mu, \quad (2)$$

with  $(t_x, t_y, t', \mu) = (0.44, 0.44, -0.14, 0.50)\text{eV}$ ,  $(0.31, 0.045, 0.01, 0.24)\text{eV}$ ,  $(0.045, 0.31, 0.01, 0.24)\text{eV}$  for the  $i = xy, xz, yz$ -bands, respectively, and  $t_{\perp}$  reflecting the hybridization between the *xz* and *yz*-bands [19]. After diagonalizing the Hamiltonian, Eq.(1), we obtain the energy dispersions for the  $\gamma$  and hybridized  $\alpha$  and  $\beta$ -bands

$$\epsilon_{\alpha, \beta}(\mathbf{k}) = \epsilon_{\mathbf{k}}^{\pm} \mp \sqrt{(\epsilon_{\mathbf{k}}^{-})^2 + t_{\perp}^2}, \quad \epsilon_{\gamma}(\mathbf{k}) = \epsilon_{\mathbf{k}}^{xy}, \quad (3)$$

with  $\epsilon_{\mathbf{k}}^{\pm} = (\epsilon_{\mathbf{k}}^{xz} \pm \epsilon_{\mathbf{k}}^{yz})/2$ . By fitting the area and shape of the  $\alpha$  and  $\beta$ -FS to those observed by ARPES [15] and dHvA experiments [16], we obtain  $t_{\perp} \approx 0.1$  eV; the Fermi surfaces for all three bands are shown in Fig. 1.

The superconducting gap for unitary spin triplet pairing can be written as

$$\Delta_{\zeta\eta}(\mathbf{k}) = [\mathbf{d}(\mathbf{k}) \cdot \sigma i \sigma_2]_{\zeta\eta} \quad (4)$$

where  $\sigma$  are the Pauli matrices. We assume that spin-orbit coupling locks the  $\mathbf{d}$  vector along the crystal  $\hat{c}$  axis,

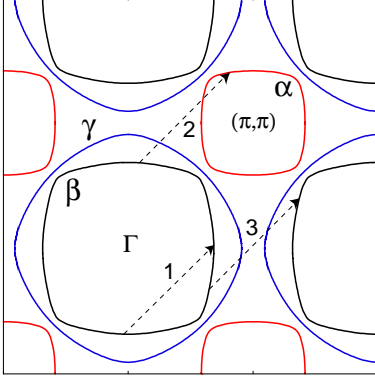


FIG. 1. Fermi surfaces of  $\text{Sr}_2\text{RuO}_4$  in the extended Brillouin zone. The arrows show quasiparticle excitations with nesting wavevector  $\mathbf{Q}_i \simeq (0.72\pi, 0.72\pi)$  where we set the lattice constant  $a = 1$ .

*i.e.*,  $\mathbf{d} \parallel \hat{z} \parallel \hat{c}$ , consistent with KS [4] and ENS [5] experiments. In the following, we consider a superconducting gap with ‘ $f_{xy}$ -wave’ ( $E_u$ ) symmetry,

$$d_z(\mathbf{k}) = \Delta(\mathbf{k}) = \Delta_0 \sin k_x \sin k_y (\sin k_x + i \sin k_y) , \quad (5)$$

which was shown [20] to be consistent with the low temperature power laws observed in specific heat and thermal conductivity experiments. Our conclusions are, however, insensitive to the detailed form of the gap function for triplet pairing. We take  $\Delta_0 \approx 1$  meV as reported by Andreev point-contact spectroscopy [21].

For spin triplet pairing, and isotropic spin fluctuations, the unrenormalized band susceptibility,  $\chi$ , is given by [22]

$$\chi_{ij}^{rs}(\mathbf{p}) = -\frac{1}{2} \sigma_{\zeta\eta}^i \sigma_{\tau\delta}^j T \sum_{\mathbf{k}, m} \mathcal{A}_{\mathbf{k}, \mathbf{q}}^{rs} \left\{ G_{\eta\tau}^r(\mathbf{l}) G_{\delta\zeta}^s(\mathbf{l} + \mathbf{p}) - [F_{\zeta\tau}^r(\mathbf{l})]^* F_{\eta\delta}^s(\mathbf{l} + \mathbf{p}) \right\} , \quad (6)$$

where  $r, s = \alpha, \beta, \gamma$  are band indices,  $\mathbf{p} = (\mathbf{q}, i\omega_n)$ ,  $\mathbf{l} = (\mathbf{k}, i\nu_m)$  are four-vectors, and

$$G_{\eta\tau}^r(\mathbf{l}) = -\delta_{\eta\tau} \frac{i\nu_m + \epsilon_r(\mathbf{k})}{\nu_m^2 + E_r^2(\mathbf{k})} , \quad F_{\eta\tau}^r(\mathbf{l}) = \frac{\Delta_{\eta\tau}(\mathbf{k})}{\nu_m^2 + E_r^2(\mathbf{k})} , \quad (7)$$

are the normal and anomalous Greens functions, respectively, with  $E_r(\mathbf{k}) = \sqrt{\epsilon_r^2(\mathbf{k}) + |\Delta_{\mathbf{k}}|^2}$  [23]. The hybridization between the bands is reflected in

$$\mathcal{A}_{\mathbf{k}, \mathbf{q}}^{rs} = \frac{1}{2} \pm \frac{\epsilon_{\mathbf{k}}^- \epsilon_{\mathbf{k}+\mathbf{q}}^- + t_{\perp}^2}{2\sqrt{(\epsilon_{\mathbf{k}}^-)^2 + t_{\perp}^2} \sqrt{(\epsilon_{\mathbf{k}+\mathbf{q}}^-)^2 + t_{\perp}^2}} , \quad (8)$$

where the upper (lower) sign applies to  $rs = \alpha\alpha, \beta\beta$  ( $rs = \alpha\beta, \beta\alpha$ ),  $\mathcal{A}^{\gamma\gamma} = 1$ , and  $\mathcal{A}^{rs} = 0$  otherwise. In what follows we distinguish between  $\chi_{ij}^{hyb} = \chi_{ij}^{\alpha\alpha} + \chi_{ij}^{\beta\beta} + 2\chi_{ij}^{\alpha\beta}$ ,

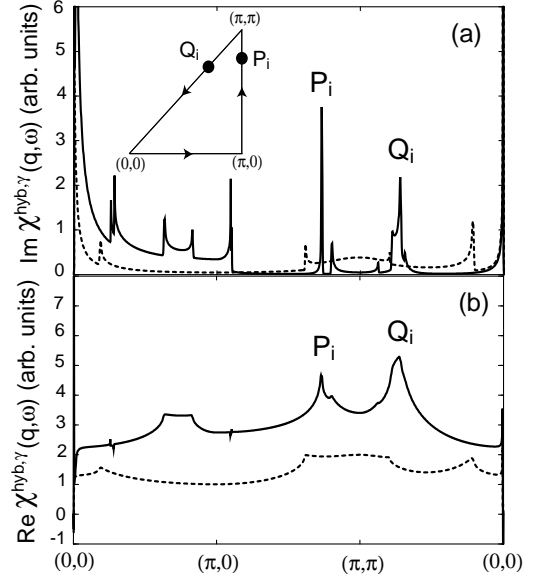


FIG. 2.  $\mathbf{q}$ -scans of (a)  $\text{Im } \chi_{NS}^i$ , and (b)  $\text{Re } \chi_{NS}^i$  for  $i = \text{hyb}$  (solid line) and  $i = \gamma$  (dashed line) at  $\omega = 6.0$  meV and  $T = 1.0$  meV. Inset (a): Path of  $\mathbf{q}$ -scan with filled circles showing wavevectors  $\mathbf{Q}_i$  and  $\mathbf{P}_i$ .

which arises from intra- and interband quasiparticle transitions in the  $\alpha$  and  $\beta$ -bands, and  $\chi_{ij}^{\gamma} \equiv \chi_{ij}^{\gamma\gamma}$  due to quasiparticle excitations in the  $\gamma$ -band. Note that the out-of-plane,  $\chi_{zz}(\mathbf{p})$ , and in-plane susceptibility,  $\chi_{\pm}(\mathbf{p})$ , differ in the form of their superconducting coherence factors, which as we show below, gives rise to their *qualitatively* different frequency and momentum dependence. Finally, the bare susceptibility, Eq.(6), in correlated electron systems is renormalized by an effective quasiparticle interaction,  $U$ , and one has in random-phase approximation (RPA), neglecting vertex corrections

$$\bar{\chi}_{ij}^{hyb, \gamma} = \chi_{ij}^{hyb, \gamma} \left( 1 - U \chi_{ij}^{hyb, \gamma} \right)^{-1} . \quad (9)$$

In Fig. 2 we present the normal state susceptibility,  $\chi_{NS} = (\chi_{zz} + 2\chi_{\pm})/3$ , obtained from Eq.(6) with  $\Delta_0 = 0$  for  $\omega = 6.0$  meV along the momentum path shown in the inset. In the vicinity of  $(\pi, \pi)$ ,  $\chi_{NS}^{hyb}$  exhibits peaks at  $\mathbf{Q}_i$  and  $\mathbf{P}_i$ , arising from the nesting properties of the  $\alpha$  and  $\beta$ -bands, while  $\chi_{NS}^{\gamma}$  provides only a weakly  $\mathbf{q}$ -dependent background [24]. Moreover, for  $q \rightarrow 0$  the form of  $\text{Im } \chi_{NS}^{hyb} \sim q^{-1}$  reflects the predominantly one-dimensional (1D) character of the  $xz, yz$ -bands, while  $\text{Im } \chi_{NS}^{\gamma} \sim \omega/q$  arises from the cylindrical nature of the  $xy$ -band.

In Fig. 3 we present the RPA susceptibility,  $\bar{\chi}_{NS}$ , in the normal state. A fit of our results, Eq.(9), to the measured  $\omega$ -dependence of  $\text{Im } \chi_{NS}$  at  $\mathbf{Q}_i$  (see inset) yields  $U = 0.175$  eV [25] in agreement with Ref. [13]. Due to the  $\mathbf{q}$ -structure of  $\text{Re } \chi_{NS}^{hyb}$  (Fig. 2b), and the weak  $\mathbf{q}$ -dependence of  $U$  [13],  $\text{Im } \bar{\chi}_{NS}^{hyb}$  is reduced from its bare

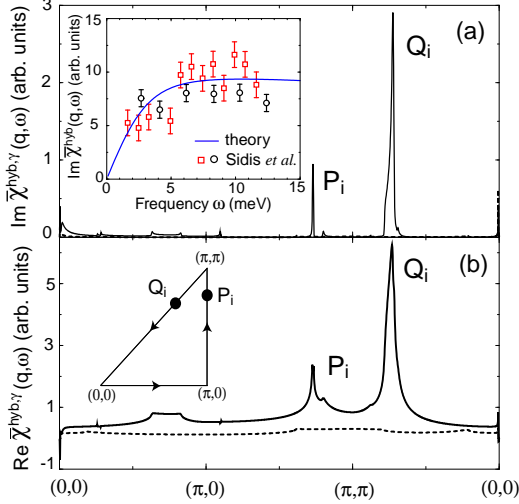


FIG. 3.  $\mathbf{q}$ -scans for  $\bar{\chi}_{NS}^{hyb}$  (solid line) and  $\bar{\chi}_{NS}^{\gamma}$  (dashed line) for the same parameters as shown in Fig. 2. Inset (a): Fit of  $\text{Im} \bar{\chi}^{hyb}$  at  $\mathbf{Q}_i$  to the data of Ref. [12];  $\text{Im} \bar{\chi}$  is multiplied by a mass enhancement factor  $m^*/m_{\text{band}} \sim 4$  in agreement with dHvA experiments [16,26].

value for small  $\mathbf{q}$ , but still possesses peaks at  $\mathbf{Q}_i$  and  $\mathbf{P}_i$ . In contrast,  $\bar{\chi}_{NS}^{\gamma}$  is strongly suppressed for all  $\mathbf{q}$ . Thus, the experimentally observed peak close to  $\mathbf{Q}_i$  arises primarily from  $\text{Im} \bar{\chi}_{NS}^{hyb}$  and the strongest SC pairing most likely occurs between electrons in the  $\beta$ -band.

In Fig. 4a we present the frequency dependence of  $\text{Im} \chi^{hyb}$  at  $\mathbf{Q}_i$  in the normal and superconducting state. There exist three channels for quasiparticle excitations with wavevector  $\mathbf{Q}_i$  which contribute to  $\text{Im} \chi^{hyb}$ , as indicated by arrows in Fig. 1. In the normal state all three channels are excited in the low frequency limit, which yields  $\text{Im} \chi_{NS}^{hyb} \sim \omega$ , in agreement with our numerical results in Fig. 4a. The dominant contribution to  $\text{Im} \chi^{hyb}$ , both in the normal and superconducting state, arises from excitations of type (3), since (a) they are intraband  $xz$  (or  $yz$ ) transitions and thus independent of  $t_{\perp}$ , and (b) the FS exhibits the largest nesting in this region of momentum space.

In the superconducting state excitations (1-3) possess nonzero threshold energies,  $\omega_{cn}$  with  $n = 1, 2, 3$ , that are determined by the momentum dependence of the order parameter and the shape of the Fermi surface. Specifically,  $\omega_{cn} = |\Delta_{\mathbf{k}}| + |\Delta_{\mathbf{k}+\mathbf{Q}_i}|$ , where  $\mathbf{k}$  and  $\mathbf{k} + \mathbf{Q}_i$  both lie on the Fermi surface, as shown in Fig. 1. For the band parameters chosen, we obtain  $\omega_{c1} \simeq 0.15\Delta_0$ ,  $\omega_{c2} \simeq 0.8\Delta_0$ , and  $\omega_{c3} \simeq 2.1\Delta_0$ . Since excitations (1-3) are well separated in frequency, we can identify their relative contribution to  $\text{Im} \chi_{zz,\pm}^{hyb}$ . While  $\omega_{c1}$  cannot be observed in the frequency dependence of  $\text{Im} \chi_{zz,\pm}^{hyb}$  due to the negligible spectral weight of excitation (1),  $\omega_{c2}$  and  $\omega_{c3}$  can clearly be identified. The large spectral weight of excitation (3) likely makes  $\omega_{c3}$  the experimentally observable

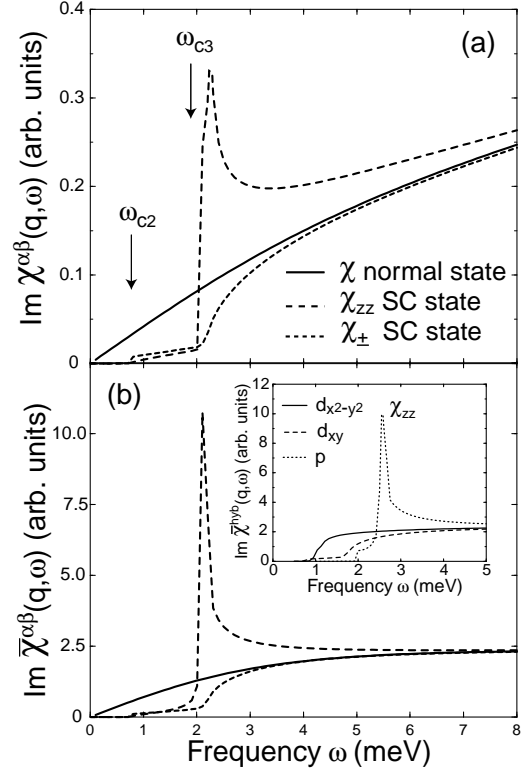


FIG. 4. Spin susceptibilities at  $\mathbf{Q}_i$  for the  $f_{xy}$ -wave state at  $T = 0$ : (a) bare susceptibility,  $\text{Im} \chi^{hyb}$ ; (b) RPA susceptibility,  $\text{Im} \bar{\chi}^{hyb}$ , for  $U = 0.175 \text{ eV}$ . The frequency integral of  $\text{Im} \chi^{hyb}(\mathbf{Q}_i)$  up to 15 meV remains constant through  $T_c$ . Inset: For spin singlet states with  $d_{xy}$  or  $d_{x^2-y^2}$  symmetry  $\text{Im} \bar{\chi}_{zz}^{hyb}$  shows *no* resonance peak, contrary to the spin triplet  $p$ -wave state.

spin gap. Moreover, due to the superconducting coherence factors which appear in the calculation of  $\chi_{zz,\pm}^{hyb}$ , the overall frequency dependence of the in-plane and out-of-plane component of  $\text{Im} \chi^{hyb}$  are *qualitatively* different. Specifically, since  $\text{Re}(\Delta_{\mathbf{k}} \Delta_{\mathbf{k}+\mathbf{q}}^*)$  is negative for transition (3), but positive for transition (2),  $\text{Im} \chi_{zz}^{hyb}$  ( $\text{Im} \chi_{\pm}^{hyb}$ ) exhibits a sharp jump at  $\omega_{c3}$  ( $\omega_{c2}$ ) and increases continuously at  $\omega_{c2}$  ( $\omega_{c3}$ ). Consequently,  $\text{Re} \chi_{zz}^{hyb}$  ( $\text{Re} \chi_{\pm}^{hyb}$ ) possesses a logarithmic divergence at  $\omega_{c3}$  ( $\omega_{c2}$ ).

In Fig. 4b we present the RPA susceptibility,  $\text{Im} \bar{\chi}_{zz,\pm}^{hyb}$ , in the superconducting state, assuming that  $U$  remains unchanged below  $T_c$ . Due to the logarithmic divergence of  $\text{Re} \chi_{zz}^{hyb}$  at  $\omega_{c3}$ ,  $\text{Im} \bar{\chi}_{zz}^{hyb}$  exhibits a *resonance* peak at a frequency slightly below  $\omega_{c3}$ . In contrast,  $\text{Im} \bar{\chi}_{\pm}^{hyb}$  increases continuously above  $\omega_{c3}$ . The logarithmic divergence of  $\text{Re} \chi_{\pm}^{hyb}$  at  $\omega_{c2}$  is rapidly smoothed out for finite quasiparticle damping due to its small prefactor and is likely experimentally not observable. Thus, we predict that for triplet pairing  $\text{Im} \bar{\chi}_{zz}^{hyb}$  and  $\text{Im} \bar{\chi}_{\pm}^{hyb}$  possess *qualitatively* different frequency dependencies at  $\mathbf{Q}_i$  with only  $\text{Im} \bar{\chi}_{zz}^{hyb}$  exhibiting a resonance peak below  $\omega_{c3}$ . In con-

trast, a resonance peak was predicted in Refs. [27,28] for the in-plane component  $\text{Im}\bar{\chi}_{\pm}$ , but not for  $\text{Im}\bar{\chi}_{zz}$ . A comparison of our results for  $\chi_{zz,\pm}$  with those in [27,28] suggests that the SC coherence factors for  $\chi_{zz,\pm}$  have been interchanged in Refs. [27,28]. We obtain the correct  $\omega, q \rightarrow 0$  limit only for the SC coherence factors which appear in our results for  $\chi_{zz,\pm}$  in Eq.(6). In this case, we find that  $\text{Re}\chi_{zz}$  decreases below  $T_c$  when a SC gap opens, while  $\text{Re}\chi_{\pm}$  remains unchanged. As shown by Leggett [30], this result is a general property of any unitary state if  $\mathbf{d}||\hat{c}$ .

We find that our results are insensitive to details of the electronic band structure or the symmetry of the gap function for spin triplet pairing. In particular, for a nodeless superconducting gap with ‘ $p$ -wave’ symmetry [2],  $\Delta(\mathbf{k}) = \Delta_0(\sin k_x + i \sin k_y)$ , belonging to the  $E_u$  representation, the frequency and momentum dependence of  $\text{Im}\bar{\chi}_{zz,\pm}^{hyb}$  remains to a large extent unchanged from that shown in Fig. 4b (see inset); a resonance peak appears again only in  $\text{Im}\bar{\chi}_{zz}^{hyb}$ . In contrast, for spin singlet pairing the in-plane and out-of-plane susceptibilities are identical and our calculations (analogous to triplet pairing) are *qualitatively* different since no resonance peak exists in  $\text{Im}\bar{\chi}^{hyb,\gamma}$ . In the inset of Fig. 4 we plot  $\text{Im}\bar{\chi}^{hyb}$  at  $\mathbf{Q}_i$  as a function of frequency for SC gaps with  $d_{x^2-y^2}$  symmetry,  $\Delta(\mathbf{k}) = \Delta_0(\cos k_x - \cos k_y)/2$ , and  $d_{xy}$ -symmetry,  $\Delta(\mathbf{k}) = \Delta_0 \sin k_x \sin k_y$ , with  $\Delta_0 = 1$  meV. In both cases,  $\text{Im}\bar{\chi}^{hyb}$  increases continuously above  $\omega_{c3}$ , since  $\Delta(\mathbf{k})$  does *not* change sign for excitation (3) and no logarithmic singularity occurs in  $\text{Re}\chi^{hyb}$ . In contrast, for the FS geometry of the HTSC and a SC gap with  $d_{x^2-y^2}$  symmetry, one finds  $\Delta_{\mathbf{k}} \Delta_{\mathbf{k}+\mathbf{Q}} < 0$ , which as described above leads to a resonance peak at  $\mathbf{Q} = (\pi, \pi)$  [29]. A resonance peak is thus *not* an intrinsic property of singlet or triplet superconductivity, but arises from the interplay of FS topology and symmetry of the SC gap.

An additional contribution to  $\chi_{\pm}$  in the SC state can in principle come from a coupling of the spin density to in-plane fluctuations of  $\mathbf{d}$ . However, for the  $\mathbf{q}$ -independent coupling assumed in Ref. [27], we find that these fluctuation contributions (FC) are three orders of magnitude smaller than those coming from Eq.(6). Moreover, the spin-orbit coupling present in  $\text{Sr}_2\text{RuO}_4$  introduces a gap for in-plane fluctuations of  $\mathbf{d}$  which further suppresses the FC to  $\chi_{\pm}$  and renders them irrelevant.

In summary, we present a scenario for the spin susceptibility in the normal and SC state of  $\text{Sr}_2\text{RuO}_4$ . In the normal state we find a peak close to the experimentally observed position at  $\mathbf{Q}_i$ . For spin triplet pairing in the superconducting state we show that the momentum and frequency dependence of  $\text{Im}\bar{\chi}_{zz}$  and  $\text{Im}\bar{\chi}_{\pm}$  are *qualitatively* different. We predict the appearance of a resonance peak in  $\text{Im}\bar{\chi}_{zz}$ , similar to the one observed in the HTSC, and its absence in  $\text{Im}\bar{\chi}_{\pm}$ . Finally, we show that no resonance peak exists for spin singlet pairing.

We would like to thank A.V. Balatsky, P. Dai and Y. Maeno for stimulating discussions. This work was sup-

ported in part through the Los Alamos Summer School and the Department of Energy.

- 
- [1] Y. Maeno *et al.*, Nature (London) **372**, 532 (1994).
  - [2] T.M. Rice and M. Sigrist, J. Phys.: Condens. Matter **7**, L643 (1995).
  - [3] G. Baskaran, Physica B **223-224**, 490 (1996).
  - [4] H. Mukuda *et al.*, J. Low Temp. Phys. **117**, 1587 (1999).
  - [5] J.A. Duffy *et al.*, Phys. Rev. Lett. **85**, 5412 (2000).
  - [6] G.M. Luke *et al.*, Nature (London) **394**, 558 (1998).
  - [7] D. Agterberg, T.M. Rice, and M. Sigrist, Phys. Rev. Lett. **78** 3374 (1997).
  - [8] S. Nishizaki, Y. Maeno, and Z. Mao, J. Phys. Soc. Jpn. **69**, 572 (2000).
  - [9] H. Suderow *et al.*, J. Phys.: Condens. Matter **10**, L597 (1998); M.A. Tanatar *et al.*, Physica C **341**, 1841 (2000).
  - [10] I. Bonalde *et al.*, Phys. Rev. Lett. **85**, 4775 (2000).
  - [11] K. Ishida *et al.*, Phys. Rev. Lett. **84**, 5387 (2000).
  - [12] Y. Sidis *et al.*, Phys. Rev. Lett. **83**, 3320 (1999).
  - [13] I.I. Mazin and D.J. Singh, Phys. Rev. Lett. **82**, 4324 (1999).
  - [14] J. Rossat-Mignod *et al.* Physica C **185-189**, 86 (1991); H. A. Mook *et al.* Phys. Rev. Lett. **70**, 3490 (1993); H.F. Fong *et al.*, Phys. Rev. Lett. **75**, 316 (1995); P. Bourges *et al.* Phys. Rev. B **53**, 876 (1996).
  - [15] A.V. Puchkov *et al.*, Phys. Rev. B **58**, R13322 (1998).
  - [16] A.P. Mackenzie *et al.*, Phys. Rev. Lett. **76**, 3786 (1996).
  - [17] I.I. Mazin and D.J. Singh, Phys. Rev. Lett. **79**, 733 (1997); A. Liebsch and A. Lichtenstein, Phys. Rev. Lett. **84**, 1591 (2000).
  - [18] The coupling of the  $\gamma$ -band to the  $\alpha, \beta$ -bands, implied by observation of a single  $T_c$ , is at the most weak and irrelevant for our results.
  - [19] We neglect the weaker nearest neighbor hopping terms between the  $xz$  and  $yz$ -bands.
  - [20] M.J. Graf and A.V. Balatsky, Phys. Rev. B **62**, 9697 (2000); Y. Hasegawa, K. Machida, and M. Ozaki, J. Phys. Soc. Jpn. **69**, 336 (2000); T. Dahm, H. Won, and K. Maki, cond-mat/0006301 (unpublished).
  - [21] F. Laube *et al.*, Phys. Rev. Lett. **84**, 1595 (2000).
  - [22] W.F. Brinkman, J.W. Serene, and P.W. Anderson, Phys. Rev. A **10**, 2386 (1974).
  - [23] We neglect interband pairing since it leads to non-zero total momentum of the Cooper pairs.
  - [24] In general,  $U$  can be different in the  $\gamma$  and  $\alpha, \beta$ -bands, however, even a value of  $U^\gamma$  twice larger than  $U^{\alpha\beta}$  does *not* substantially enhance  $\text{Im}\bar{\chi}^\gamma$ .
  - [25]  $U$  defined in Ref. [13] contains an additional factor of 2.
  - [26] C. Bergemann *et al.*, Phys. Rev. Lett. **84**, 2662 (2000).
  - [27] H.-Y. Kee, J. Phys.: Condens. Matter **12**, 2279 (2000).
  - [28] D. Fay and L. Tewordt, Phys. Rev. B **62**, 4036 (2000).
  - [29] I.I. Mazin and V.M. Yakovenko, Phys. Rev. Lett. **75**, 4134 (1995); J.P. Carbotte, E. Schachinger, and D.N. Basov, Nature (London) **401**, 354 (1999).
  - [30] A.J. Leggett, Rev. Mod. Phys. **47**, 331 (1975).